SOUND RECORDING AND REPRODUCTION

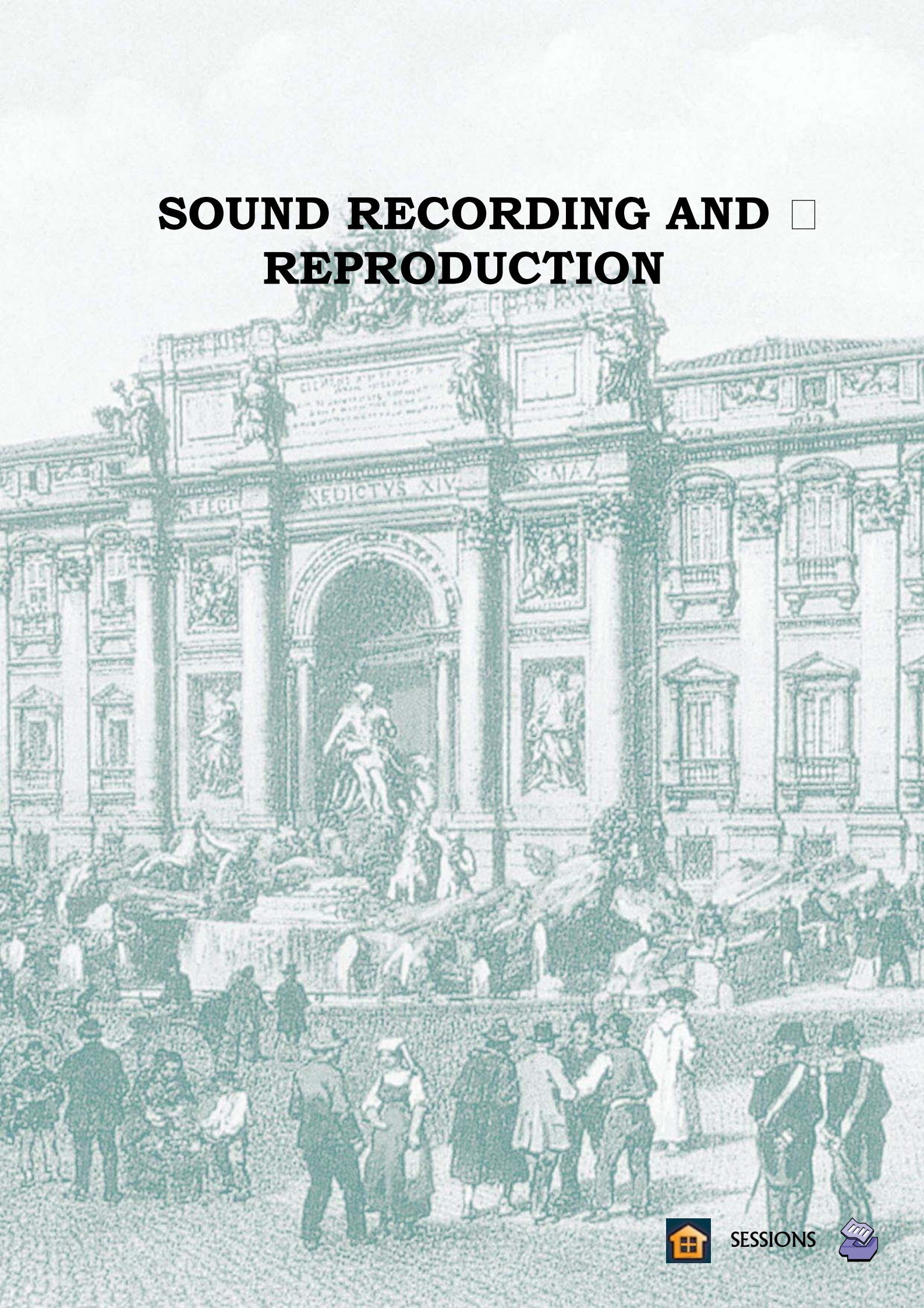

Optimization of Performance of Noise Shaping Filter for Digital Audio Power Amplifier Application

P. Kyoungsoo[a], Y. Choi[b] and K.-M. Sung[a]

[a]*School of Electrical Engineering, Seoul National University, Shillim-dong, Seoul, Korea*
[b]*Neofidelity Inc., Dearim-dong 1101-14, Seoul, Korea*

Noise shaping filter in fully digital amplifier is optimized with optimal coefficients of real number suggested. To derive the coefficients, Noise Shaping Gain is suggested as an object function of the filter performance. The enhancement of performance compared to the conventional filter with integer coefficients is analyzed and simulated. The results show that the suggested filter gives much more signal to noise ratio for a given filter order.

INTRODUCTION

Digital audio amplifier in this paper means fully digital power amplifier that accepts signal as digital format like SPDIF or IIS. Its main functional blocks consists of over sampler, noise shaper, Pulse Width Modulation (PWM) converter and power stage that amplifies the amplitude of PWM wave.

Oversampling pushes audio signal into lower band of normalized frequency but spreads noise over the entire frequency. Direct conversion of oversampled data into PWM needs too high resolution of PWM wave for high fidelity audio signal, which makes hardware implementation impossible. Therefore, requantization to reduce bit resolution of the signal is needed. However, requantization amplifies quantization noise unbearably. To avoid noise problem, noise shaping filter is used. Noise shaping filter reshapes quantization noise and the noise in the audio band is pushed into higher frequency. Most popular noise shaping filter is a form of which Noise Transfer Function (NTF) has all the zeros at 1. The coefficients of that kind of the filters are all integers. In this paper, however, optimal condition of the filter performance has suggested and the coefficients of real numbers are derived.

DERIVATION OF OPTIMAL

COEFFICIENT

General form of noise shaping filter is shown in Figure 1. Noise shaper accepts input signal with b-bit resolution and outputs the processed signal having bit resolution of b′ that b′ is smaller than b. Inside the noise shaper, the quantizer generates a requantization error signal e_{rq} by subtracting quantized signal to the original signal, which is equivalent to the truncated low-order bits of the input signal, and the spectrum of this requantization error signal is modified by a filter *H(z)* and then this frequency-shaped error signal e_{ns} is added back to the input stage to compensate and reduce requantization noise.

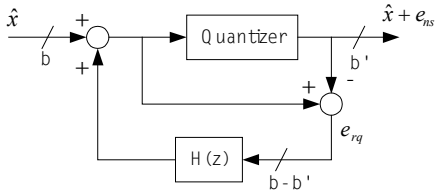

FIGURE 1 General form of noise shaping filter

The noise transfer function NTF(z) can be defined as

$$\mathrm{NTF}(z) = \frac{E_{\mathrm{ns}}(z)}{E_{\mathrm{rq}}(z)} = H(z) - 1 \qquad (1)$$

where $E_{ns}(z)$ are $E_{rq}(z)$ are the z transform of e_{ns} and e_{rq} respectively. And the conventional noise shaping filter can be represented as

$$1 - H(z) = (1 - z^{-1})^N \qquad (2)$$

where N is the filter order[1, 2]. To derive optimal coefficients, the coefficients of NTF are assumed arbitrary value.

$$\mathrm{NTF}(z) = -1 + \sum_{k=1}^{N} a_k z^{-k} \qquad (3)$$

An object function, Noise Shaping Gain is defined as the power ratio of P_s, P_{ns}, and P_{rq} where they are the power of signal, the power of shaped noise and the power of requantized noise respectably within audio frequency in digital amplifier.

$$\text{NSG} \equiv \quad 10\log_{10}\frac{P_{rq}}{P_{ns}} \tag{4}$$

Partially differentiating NSG for each a_k the simultaneous condition gives the set of real coefficients which minimize the NSG.

$$\frac{\partial \text{NSG}}{\partial a_k} = 0 \tag{5}$$

For the oversampling ratio of M, the solution of the eq. (5) is given as below,

$$\mathbf{A} = \mathbf{G}^{-1}\mathbf{B} \tag{6}$$

where $\mathbf{A} = \left(a_1, a_2, \cdots a_N\right)^T$, $\mathbf{B} = \left(b_1, b_2, \cdots b_N\right)^T$, $b_k = \frac{4}{k}\sin\frac{k\pi}{M}$ and the elements of $\mathbf{G}$ are

$$g_{mn} = \begin{cases} \dfrac{4\pi}{M} & (m = n) \\ \dfrac{4}{n-m}\sin\dfrac{(n-m)\pi}{M} & (n > m) \\ g_{nm} & (m > n) \end{cases}$$

RESULTS

From the eq. (6) the approximate optimal coefficients for 8 time oversampling ratio are given in Table 1. NSG of the integer coefficient filter and the real number optimal filter are computed and shown in Figure 2. NSG or SNR of Noise shaper with optimal coefficients is enhanced about 30dB for 7th order filter.

Computer simulation for integer coefficient filter and optimal real number filter was performed and the result is shown in figure 3. A test signal of 1kHz pure tone is entered into noise shaper with 18-bit and 8 time oversampling ratio. Noise floor of the suggested filter output is lowered about 25dB.

REFERENCES

1. J. M. Goldberg, M. B. Sandler, "Noise Shaping and Pulse-Width Modulation for an All-Digital Audio Power Amplifier",J. Audio Eng. Soc., vol.39 pp. 449-460 (1991 June).

2. Alan V. Oppenheim, Ronald W. Schafer with John R. Buck, DISCRETE-TIME SIGNAL PROCESSING 2nd ed. pp 201-213 (Prentice Hall Signal Processing Series, Upper Saddle River, New Jersey, 1999)

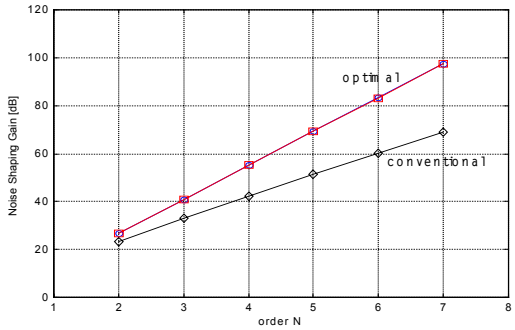

FIGURE 2 Noise Shaping Gain vs. filter order.

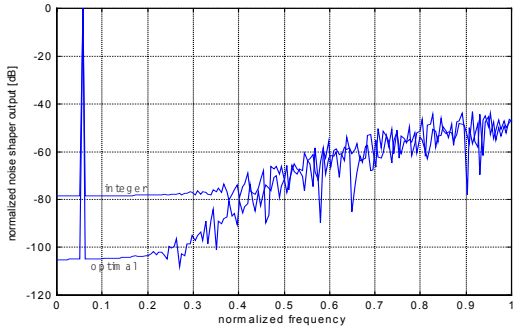

FIGURE 3 Spectrum of noise shaper output.

Table 1. Optimal coefficients of the noise shaping filter(8 time oversampling).

order	2	3	4	5	6	7
a_1	1.9290	2.8891	3.8502	4.8116	5.7732	6.7350
a_2	-0.9795	-2.8703	-5.6846	-9.4235	-14.0874	-19.6767
a_3		0.9802	3.8129	9.3872	18.5927	32.3201
a_4			-0.9805	-4.7559	-13.9971	-32.2316
a_5				0.9806	5.6991	19.5151
a_6					-0.9807	-6.6427
a_7						0.9807

Evaluation of different methods for room/loudspeaker equalization

A. Landragin[a], S. Debusne[b], S. Javelot[b], D. Lebrun[b], G. de Rivoyre[a] and J. Lewiner[b]

a- Cynove, 35 rue Tournefort, 75005 Paris, France

b- Laboratoire d'Electricité Générale, Ecole Supérieure de Physique et de Chimie Industrielles de la Ville de Paris, 10 rue Vauquelin, 75005 Paris, France

Three different methods dedicated to room/loudspeaker equalization have been developped and compared : real-time adaptive filtering, wavelet decomposition, and dereverberation echoes deconvolution. First, experimental room/loudspeaker impulse responses have been recorded using a precision microphone and a 24 bits acquisition unit. Second, different algorithms have been tested in simulation runs on the recorded signals for each of the above method.

INTRODUCTION

When an electrical pulse signal *x(t)* is sent to a loudspeaker system, in a reverberant room, the acoustic response is distorted, on the one hand, because of its natural response, and on the other hand, because of echoes. The sound pressure *p(t)* at a listening position can be expressed as :

$$p(t)=a_0(t)x(t-t_0)+...+a_n(t)x(t-t_n)+b(t) \quad (1)$$

Where $a_0(t)$ is the response function to the direct signal, $a_i(t)$ and t_i are respectively the response functions for each echoes and the corresponding time of arrival and *b(t)* a noise that is supposed to have a white gaussian spectrum. To retrieve a pressure proportional to the original signal *x(t)*, three methods are presented, using adaptive filtering, wavelet decomposition, and deconvolution. In each case we choose to determine a filter of response *w(t)* such that :

$$p(t)\otimes w(t)=i(t)\otimes x(t) \quad (2)$$

where $\otimes$ is the convolution operator and *i(t)* the identity function.

We will successively describe the theoretical equalization methods, the results which have been obtained, and conclude.

EQUALIZATION METHODS

Real-time adaptive filtering

In fig.1, we show a block diagram of the method. The electrical signal at the output of the measuring microphone M is *swx(t)*. The method consists in minimizing the difference between sent electrical signal *x(t)* and received signal *swx(t)*.

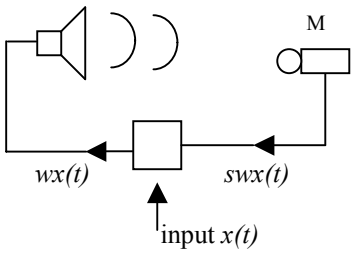

FIGURE 1. Block diagram of adaptive filtering.

We define *e(t) = x(t) – swx(t)*, and introduce the cost-function $\Sigma|e(t)|^2$. The filter *w(t)* which verifies (2) is calculated by minimizing this function [1].

A compromise had to be reached in order to make compatible two conflicting situations. Firstly in order to have a sufficient correction, the sampling frequency has to be at least five times the maximum frequency to be corrected. This implies that only low frequencies are well corrected (fig.3). Secondly, the number of computation steps for real time adaptive filtering is about ten times higher than a simple convolution with a fixed filter. This implies a much more sophisticated electronic system and thus more difficulties to implement this correction in an embedded system. For this reason we decided not to use this method.

Wavelet decomposition and deconvolution

The idea is to simulate a deconvolution of the received signal, with a Dirac comb function, using Wiener filtering [2], and to decompose the result in

wavelets, whose main aim is to decrease noise. This function is evaluated by means of the delays given by an autocorrelation method, which consists in recovering the signal by itself [3]. In this case the chosen wavelets are based on quadrature filters [4].

The output *r(t)* of the measuring microphone can be decomposed on a wavelet basis as $\tilde{r}(t)$

$$\tilde{r}(t)=\sum_{j=L+1}^{J}\sum_{m=0}^{2^{-j}}\langle r(t),\Psi_{j,m}\rangle\Psi_{j,m}+\sum_{m=0}^{2^{-J}}\langle r(t),\Phi_{J,m}\rangle\Phi_{J,m} \quad (3)$$

$< >$ represents scalar product, $\Psi_{j,m}$ and $\Phi_{J,m}$ the different wavelet and scaling functions.

Simulations have been performed using Matlab software. As will seen in Fig. 4, the first echoes are reduced, but not enough to have a significant improvement.

Dereverberation echoes deconvolution

In this case, we use (1) to express the sound pressure *p(t)* at the listening position. Firstly, we determine the various delays t_i by an autocorrelation method [3]. Secondly, we build the filter *w(t)* required to solve (2). This is done by splitting the signal *r(t)* supplied by the microphone into elementary signals $r_i(t)$, an echo one corresponding to the direct signal and the others to the following echoes. In Fig 2. we can see the direct signal and the first echoes.

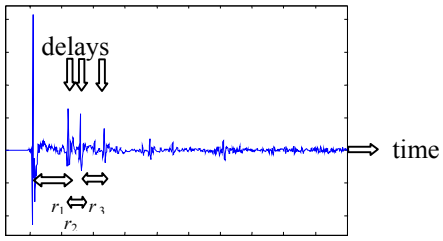

FIGURE 2. Split of the recorded signal *r(t)*

The resulting value for *w(t)* defines the optimal filter as will be seen in Fig 5.

RESULTS

Figures 3, 4, 5 show the simulated results obtained for each of the three methods.

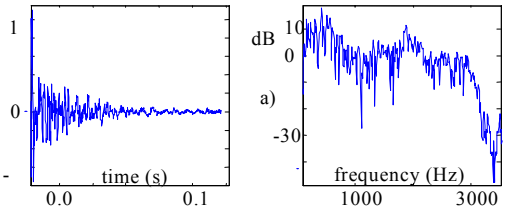

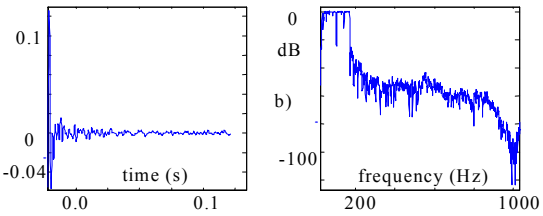

FIGURE 3. Real-time adaptive filtering. a) received signal in time and in frequency domains. b) same after equalization. As can be seen, the method does not lead to satisfactory results.

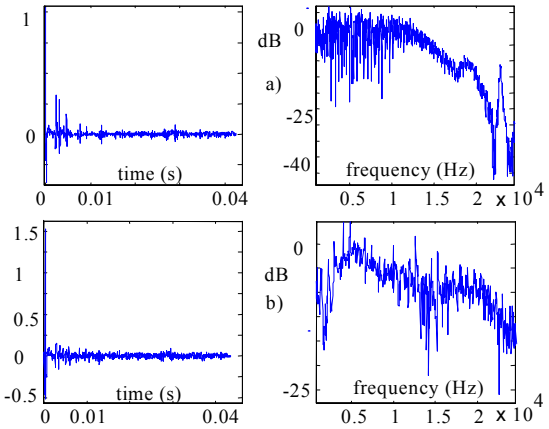

FIGURE 4. Wavelet decomposition. a) received signal in time and in frequency domains. b) same after equalization.

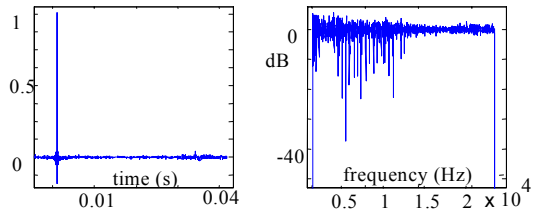

FIGURE 5. Effect on signal of Fig 4a of the deconvolution equalization. As can be seen this method leads to highly improved results.

CONCLUSION

The above results show that the deconvolution method leads to a much better equalization than real-time adaptive filtering and wavelet decomposition. The quality of the loudspeaker system can thus be dramatically increased.

REFERENCES

1. Kuo, S.M., and Morgan, D.R., *Active Noise Control Systems*, Wiley Interscience, 1998, ISBN 0-471-13424-4.
2. Hunt, B.R., *IEEE Trans., Automatic Control*, 703-705 (1972).
3. Knapp, C.H., Carter, G.C., *IEEE Trans. On Acoustics, Speech, and Signal Processing*, vol. ASSP-24, 4, 320-326 (1976).
4. Mallat, S., *A Wavelet Tour of Signal Processing*, Academic Press, 1998, pp. 246, 425-480, ISBN 0-12-466605-1.

Analysis and prototype measurements of a transmission line loudspeaker

B. Pueo and M. Romá

Department of Physics, System Engineering and Signal Theory,
University of Alicante, E-03080 Alicante, Spain

The Transmission Line Loudspeaker (TL) is a long wave guide system in which the phase of the driver's rear output is reversed, reinforcing the bass frequency range. It is designed to be 1/4-wavelength long at the free air resonance frequency of the driver, so that the acoustical output radiated from the line opening or mouth mixes with the front-wave from the driver. The analysis and design of any acoustic system is based on mathematical models. Unlike sealed and ported speaker systems, the transmission line system has never been completely and successfully modelled. In this paper, a mathematical model is tested [1] in which the classical elements of the equivalent circuits applied by Thiele and Small are used together with a specific acoustic impedance that models the pipe behaviour. The influence of the main parameters -line lengths or alignment frequencies, cross sectional areas and stuffing densities- has been evaluated by using this model. Finally, a transmission line prototype for testing and measuring was fabricated to correlate the model against some test results.

INTRODUCTION

In a Transmission Line (TL), the sound wave from the rear side of the speaker is channelled through a long pathway filled with a damping material. In a TL, very low frequencies exit the end of the tube, extending the low frequency response one half octave below the driver's resonance frequency.

PROCEDURE AND MEASUREMENTS

Before starting the experiments, an accurate test to determinate de Thiele/Small parameters of the chosen driver was made. Then, an extremely rigid prototype, made of an ultra high-density particleboard, was fabricated. To evaluate the degree in which the three main parameters affect the performance, the transmission line was fully modular. In this way, five lengths were estimated, whose resonance frequencies are third octave harmonically related: 2.62m (32,7Hz, driver's f_s), 2.08m (41.2Hz), 1.65m (51.9Hz), 1.31m (65.4Hz) and 1.04m (82.4Hz). In the same way, three cross sectional areas were evaluated: $2.2S_D$, $3S_D$, and $5S_D$. Finally, the absence of stuffing and four packing densities were investigated: 1.5, 3, 5, and 8 kg/m^3.

Since there is no acceptable mathematical model to describe the acoustic impedance seen by the driver, the most important data to take in account was the electrical impedance, closely correlated with the acoustic one. First, line length is investigated: Figure 1 shows that the relation between the experimental impedance peak frequencies and the computed quarter wavelength frequencies remains constant as the line length increases. Also, independently of any cross sectional area, the greater the ¼ wavelength resonance, the greater the speaker impedance peak whereas the smaller the λ/4 mode peak. If the line length would continue decreasing, a free radiating condition would appear, described by a typical impedance curve with a maximum located at the speaker resonance (Figure 2).

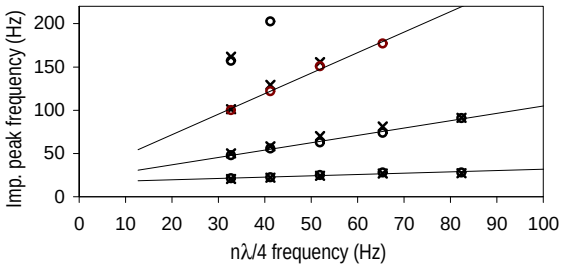

FIGURE 1. Experimental impedance peak frequencies vs. calculated quarter wavelength frequencies (X $2.2S_D$, O $3S_D$)

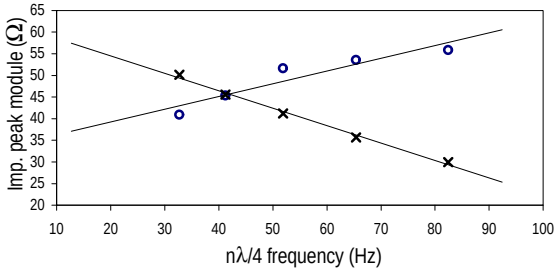

FIGURE 2. Experimental impedance peak modules vs. calculated quarter wavelength frequencies (X λ/4 mode mean value, O speaker resonance mean value)

Next, the cross sectional area is examined through the TL cross sectional area and speaker area ratio S_0/S_D for different line lengths. As shown in Figure 3, there is an opposite behaviour of the modules and frequencies of the impedance peaks. The larger the ratio S_0/S_D, the greater the speaker and the $n\lambda/4$ modes. On the contrary, as S_0/S_D increases, the $n\lambda/4$ modes approach to the speaker resonance. Extending this tendency to the limit, a TL with an infinite S_0/S_D, would behave like a speaker in an infinite baffle.

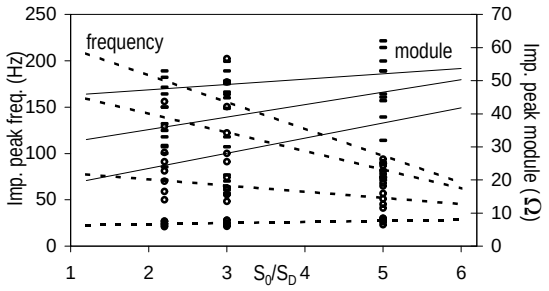

FIGURE 3. Experimental impedance peak modules and frequencies vs. the cross sectional area-speaker area ratio

Finally, the influence of the stuffing density is considered. A 1.16 g/m^3 dense 4-hole cross section polyester fibre was used instead of fibre wool to avoid the inherent problems associated with mineral wool, while preserving the required damping. Figure 4 displays a slight trend of the impedance module and frequency peaks as the packing density is augmented. A slight decrease of the speaker impedance frequency peak and an evident fall in the λ/4 mode peak is observed, while some authors argue that both frequency peaks remain constant as density increases [1]. The behaviour of the modules is quite different: as density is augmented, the speaker resonance magnitude decreases whereas, surprisingly, the first mode remains constant.

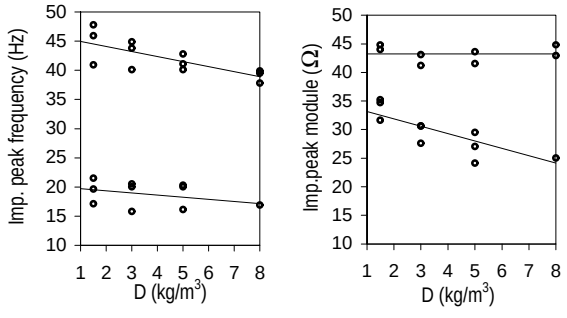

FIGURE 4. Experimental impedance peak modules and frequencies vs. stuffing material packing densities.

The second set of measurements was the SPL response at both ends of the tube, the speaker and the mouth response. The frequencies that exhibit a sharp null do not coincide with the ones in the impedance peaks, but with the calculated ¼ modes, as we might expect. Notwithstanding, the shape of the SPL response is close to the impedance shape but with a slight shift in frequency.

CONCLUSSION

The mathematical model proposed in [1] does not correlate with the expectations. More precisely, the general shapes of SPL and impedance plots agree with theory, but the position of the maximum and minimum are shifted in frequency.

Table 1. Calculated versus measured impedance resonance peaks and speaker sound pressure nulls for different quarter wavelength lengths.

Eff. line lengths	2.69m	2.15m	1.7m	1.4m	1.1m
Speaker	10.8 21	11.9 22	13.1 24	14.3 27	15.6 27
λ/4 mode	#31.9 ✠50 ⬩29.5	39.9 59 38.8	50.4 70 49.1	61.2 81 69.8	78 91 77.2
3λ/4 mode	95.6 101 95.9	119 129 112.2	151.3 156 148.9	183	234

First row: Theoretical values
✠ Second row: Impedance peak values
⬩ Third row: SPL null values

The quarter wavelength modes after including an end correction to the line length corresponding to an unflanged exit boundary condition together with the measured data are shown in Table 1. Observing the first mode, there is a constant shift in frequency of about 20 Hz, which do not change when the cross sectional area changes. The driver resonant frequency of 33 Hz dropped to 21 to 27 Hz when inserting in the TL. Assuming that this drop in frequency is due to an additional mass loading on the rear part of the speaker cone, like the delta mass technique to test the speaker V_{AS} [2], the calculated values disagree with theoretical ones.

REFERENCES

1. King, M. J., "Derivation and correlation of a viscous damping model used in the design of a transmission line loudspeaker system", personal report, New York, 2000.

2. D'Appolito J., *Testing loudspeakers*, Audio Amateur Press, Peterborough, 1998, pp. 29-30.

Interactions of (two) Closed-box Loudspeaker Systems

V. Adam

Laboratory of Electromagnetics and Acoustics (LEMA), Swiss Federal Institute of Technology (EPFL), 1015 Lausanne, Switzerland

The aim of this paper is to predict whether the interactions between two electrodynamic loudspeakers mounted in closed box have to be taken into account during the design phase. The study comprises a theoretical part involving modelling and calculation and an experimental validation part. Based on Thiele & Small parameters, Huygen's principle, geometric theory of diffraction and unified theory of diffraction, the calculations enable input impedance, volume velocity, near and far field sound pressure at all points in space, as well as force and radiation impedance to be obtained for each loudspeaker. They also enable first order modifications of loudspeaker behaviour in modulus and phase to be predicted. An experimental part is then carried out in order to validate the study.

INTRODUCTION

Within the framework of a project concerning active noise control outdoors, the specifications of the anti noise sources (electrodynamic loudspeakers mounted in closed boxes) contained an essential characteristic relating to the linearity of the phase response.

In a preliminary work [4], the analysis and synthesis of closed-box loudspeakers were studied taking into account the quality of their phase responses. A second study [5] consisted in observing whether the effect of an external sound field on a driver mounted in an infinite baffle introduced significant phase and amplitude errors. The aim was to determine which kind of measurement was the most suitable. Being located at loudspeaker terminals, the electrical quantities offered the advantage of being easily measurable. That's why these effects were measured as modifications of the system input impedance and volume velocity (sound pressure in box in so far as the latter behaves like an acoustic compliance). Highlighting a simple method of calculation and measurement, the conclusion would tend to demonstrate that these effects should not be neglected.

In the same way, this paper is about to determine whether the mutual effect between two loudspeakers has to be taken into account during the design phase. We shall first of all analyse the behaviour of two loudspeakers mounted in an infinite baffle, then in a reduced baffle and finally without any baffle. In each case the study comprises a theoretical part and an experimental validation part in an anechoic chamber.

THEORETICAL PREDICTIONS

The design of a loudspeaker is generally based on its equivalent acoustical circuit determined from Thiele & Small parameters [1]. This representation, valid in the low-frequency range, enables the membrane volume velocity to be readily calculated from input voltage as a function of frequency. The computation of the sound pressure, given as function of the system velocity, is carried out without using the radiated acoustic power, with the distinctive advantage of obtaining the phase response of the system. The theory related to loudspeaker mounted in infinite baffle is based on the Huygens principle, in which the driver is assumed to behave like a flat membrane mounted in a rigid baffle. The force and radiation impedance are then calculated according to the sound pressure in the immediate vicinity of the driver membrane.

Taking into account interactions between the sources LS_0 and LS_1, the modifications are analysed in terms of forces, which lead to volume and input impedance variations. A discrete approach is chosen in order to minimize computation time considering the fact that calculations must be fine tuned in such a way as to ensure sufficient accuracy corresponding more or less to the measurements uncertainties. This implies a double subdivision of both surfaces, taking care to avoid elements superpositions.

In the case of a reduced baffle, the diffraction at the wedges has now to be taken into account. According to Keller's geometric theory of diffraction (GTD), the total sound pressure may be directly calculated by adding direct and diffracted waves. Vanderkooy [2] showed that the diffraction contributions depend on the observation angle and explained that a phase reversal phenomenon in the illuminated zone has now to be taken into account. He limited his theory for observation angle below 130 degrees. The scope of the application related to this approximate theory is restricted to wavelength much smaller than source and distances. However, we shall see that the frequency range may be widely extended downwards.

In the case of two distant closed-box drivers, the latter theory can not be applied, due to the infinite diffracted contributions for observation points located

close to the shadow boundaries. This problem was solved by a new method called the uniform theory of diffraction (UTD) [3].

EXPERIMENTAL VALIDATIONS

Comparisons between measured and calculated LS_0 modifications according to frequency are carried out with U_1/U_0 = 10 and a distance between driver centers equal to two membrane radius. The calculation accuracy requires some preliminary measurements; then, in addition to the TS's parameters of each driver, the measured function $\underline{U}_1/\underline{U}_0$ is also introduced in calculation data (polynomial approximation of order 25).

The figure below show the LS_0 input impedance modifications in modulus and phase according to the frequency.

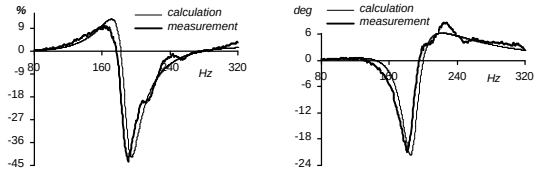

FIGURE 1. Input Impedance modifications - infinite baffle

The calculations for two loudspeakers mounted in a reduced baffle are completed by the geometric theory of diffraction, in which the wedges, made up of the both adjacent enclosures, are divided into discrete elements. The volume velocity modifications are also compared (see Fig.3). For two distant closed-box loudspeakers the GTD is modified in UTD in order to calculate the diffraction close to the shadow boundaries.

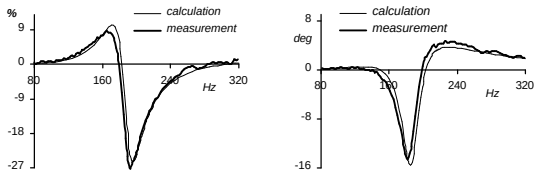

FIGURE 2. Input Impedance modifications - reduced baffle

The input impedances are modified in the order of 50% and 25 degrees for two drivers in an infinite baffle, 35% and 20 degrees for the two drivers in the reduced one, and 20% and 12 degrees for two closed-box drivers 10 cm from each other. Comparisons show that the orders of magnitude are higher at the system resonance than away from it. In the latter frequency range, the volume velocity modifications are still quite significant. The modifications vary according to parameters such as excitation voltage ratio, phase difference and distance between source centres.

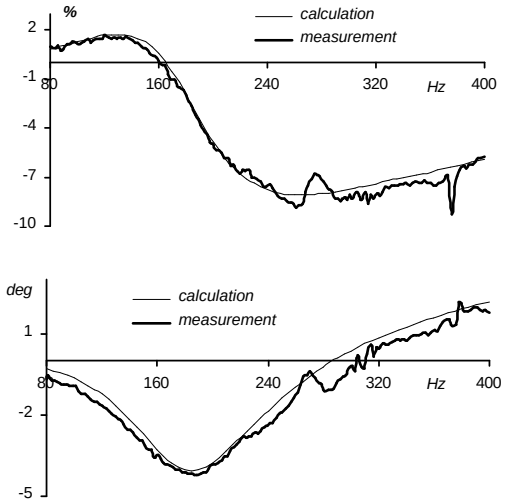

FIGURE 3. Volume velocity modifications - reduced baffle

CONCLUSION

The results show good similarities between calculated and measured modifications. The small differences come from measurement uncertainties (equipment accuracy, Matlab processing, phase reference of volume velocity, box net volume) as well as from calculation hypotheses (uniform membrane velocity, membranes subdivisions, drivers radius, measured TS's parameters).

ACKNOWLEDGMENTS

The work presented here was supported by the Swiss Federal Education and Science Institute (OFES).

REFERENCES

1. Rossi, M., *Acoustics and Electroacoustics*, Artech House, 685 Canton Street Norwood, MA 02062, 1988.
2. Vanderkooy, J., *J.A.E.S* **39(12)**, 923-933 (1991).
3. Stutzman, W.L., Thiele G.A., *Antenna Theory and Design*, John Wiley and Sons, USA, 1981.
4. Adam, V., "Amplitude and Phase Synthesis of Loudspeaker Systems", *108th AES*, Paris, preprint 5161 (2000).
5. Adam, V., "Comportement d'un Haut-parleur Soumis à un Champ Extérieur", *5th CFA*, Lausanne, 660-663 (2000).

A New Hybrid Kalman/VFF Kalman Decision Feedback Equalizer for Time-varying Channel Estimation

S.-W. Lee[a], J.-J. Jun[b], J.-S. Lim[c], S.J. Baek[b], and K.-M. Sung[b]
[a]*LG Electronics Co., Anyang,, Korea*
[b]*School of Electrical Engineering and Computer Science, Seoul National University, Seoul, Korea*
[c]*Department of Electronics Engineering, Sejong University, Seoul, Korea*

Time-varying channel, which models transmission media when transmitter or receiver is moving, is the main cause of data distortion in underwater communication system. Recently, results on adaptive Kalman equalizer with LMS channel estimator have been proposed. However, due to the inherent slow convergence speed of LMS algorithm, this type of channel estimator is known to be inefficient when channel varies very fast. To achieve the guaranteed speed of convergence, fast converging algorithm such as Kalman filtering can be applied to the tracking of channel parameters. Conventional Kalman filter, however, has the disadvantage that it has to predetermine the optimal forgetting factor according to the channel conditions. In this paper, we introduce VFF(Variable Forgetting Factor) Kalman filter as a channel estimator. The performance of the proposed method is verified through computer simulations. Results show that the proposed method outperforms the conventional one in view of mean-square-identification-error (MSIE) of time-varying channel.

INTRODUCTION

Analogue channel is the cause of corruption and transformation of input signal[1]. In radio and underwater channels, ISI is caused mainly due to multipath signal propagation, which may be viewed as transmission through a group of channels with different relative amplitudes and delays[1],[2]. In a broad sense, the term "equalizer" applies to any signal processing device designed to deal with ISI which is the distortion caused by the overlap of the received signal. One special requirement of underwater channel equalizer is that they should be able to track the time-varying fading characteristics, which are typically encountered.
In this paper, we present a new underwater channel estimation method that adopts the VFF Kalman filtering. The proposed method updates the appropriate forgetting factor at each iteration step and hence, does not need a predetermined constant forgetting factor.
MSIE performance of proposed estimator will be compared with that of conventional method by computer simulation.

Adaptive kalman dfe with lms channel estimator

Detailed structure of adaptive Kalman DFE(Decision Feedback Equalizer) can be seen in [2]. Here we skip the overall review of the DFE structure and only focus on the state space model and channel estimator model. The channel can be modeled as an FIR filter, through which the signal can be represented in the state space form as[2]

$$\mathbf{s}(k+1) = \mathbf{F}(k+1\,|\,k)\mathbf{s}(k) + \mathbf{b}s(k) \quad (1)$$

The combined observation equation is

$$\mathbf{x}(k) = \mathbf{H}\mathbf{s}(k) + \mathbf{N}(k) \quad (4)$$

where $\mathbf{H}$ is the $(d+1)\times 2$ channel matrix which is given by

$$\begin{bmatrix} \mathbf{h}^T & 0 \\ 0 & 1 \end{bmatrix} = \begin{bmatrix} h_0 & h_1 & \cdots & h_{M-1} & 0 & 0\cdots 0 \\ 0 & 0 & \cdots & 0 & 0 & 0\cdots 1 \end{bmatrix}^T . \quad (5)$$

and $\mathbf{x}(k) = [x_1(k)\ \ x_2(k)]^t$, $\mathbf{N}(k) = [n(k)\ \ 0]^t$
The LMS channel estimator can be summarized as follows.

$$\begin{aligned} \mathbf{h}(k+1) &= \mathbf{h}(k) + 2\mu\mathbf{s}(k+1)e(k+1) \\ e(k+1) &= x(k+1) - \mathbf{h}^T(k)\mathbf{s}(k+1) \\ \sigma_n^2(k+1) &= (1-1/M)\sigma_n^2(k) + e^2(k+1)/M \end{aligned} \quad (6)$$

Optimal forgetting factor and vff

LMS channel estimator cannot track the channel characteristics appropriately since the tracking speed of LMS is relatively slow. Identification of a fast-fading mobile channel has been reported in some papers [1][3]. However, the channel estimator has not yet been implemented using the VFF Kalman filter. In this section, we implement the channel estimator using VFF Kalman filter and see how the proposed equalizer works in fading channel environments.
For given fading channel, optimum forgetting factor proposed by Lin[4] is given by

$$\lambda_{opt} = 1 - \left(\frac{2\omega_D^2 E_s}{L\sigma_n^2} \right)^{\frac{1}{3}} \quad (7)$$

where ω_D is maximum Doppler frequency, E_s is average energy of signal, L is the number of the channel paths, and σ_n^2 is variance of additive noise[4].

In [5], we can find the update equations for forgetting factor as follows

$$\lambda(k) = 1 - \frac{R^{-1}(k)}{J_1^+} e^2(k)[1 - \mathbf{H}^T \mathbf{K}(k)]^2 \quad (8$$

where $R(k)$ is the variance of additive noise, J_1' is the first cost function value initiated, $e(k)$ is an estimate error, $\mathbf{K}(k)$ is Kalman gain. As a result, channel estimator (6) is replaced with Kalman filter which uses forgetting factors such as (8).

Results

Simulations were performed to compare the result of LMS, Kalman filter with various forgetting factor including optimum value and VFF Kalman filter in fast fading channel estimation. We assumed that transmitter is moving at either 20 knots or 30 knots with center frequency 50kHz and 20 kHz, respectively. The Doppler frequency corresponds to 343Hz and 205Hz for each case. The Rayleigh frequency-selective fading channel model is used for each Doppler frequency[1]. MSIE for each estimator is plotted with various SNR range in fig. 1 and in fig. 2. We can see that the proposed method has significantly low MSIE for almost every SNR in both figures compared to other estimator.

CONCLUSION

In this paper, we proposed VFF Kalman estimator to improve underwater channel estimation performance. Simulation results show that the proposed method outperforms the other types of channel estimator. This method can be applied to adaptive antenna array to estimate the DOA of the signal.

REFERENCES

1. J. G. Proakis, *Digital Communication*. New York: McGraw-Hill, 1989.

2. S. McLaughin, "Adaptive equalization via Kalman filtering technique," *Proc. IEE* vol. 138, no. 4, pp.388-396, 1991.

3. I. D. Landau, "A survey of model reference adpative techniques-Theory and applications," *Automatica*, vol. 10, pp.353-379, 1974.

4. Jingdong Lin, John G. Proakis, Fuyun Ling, and Hanoch Lev-Ari, "Optimal Tracking of Time-Varing Channels:A Frequency Domain Approach for Known and New Algorithms," IEEE trans. Selected areas in communications, Vol. 13, No. 1, January 1995.

5. S. W. Lee et al., "Time-varying signal frequency estimation by VFF Kalman filtering," *Signal Processing*, vol. 77, 343-347, 1999.

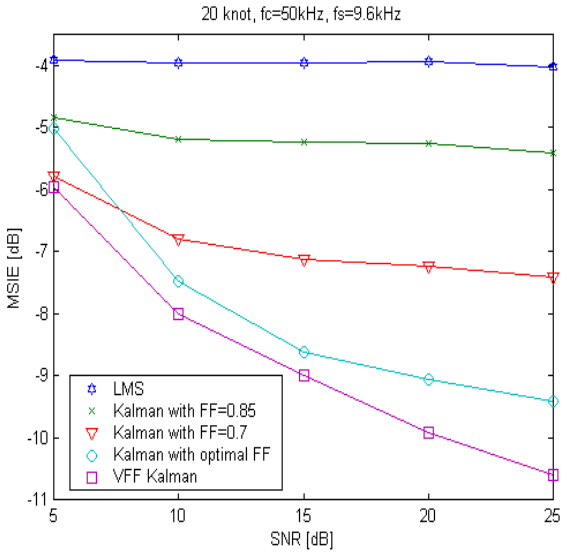

Fig. 1. MSIE comparision
(fc=50kHz, fs=9.6kHz, v=20 knots)

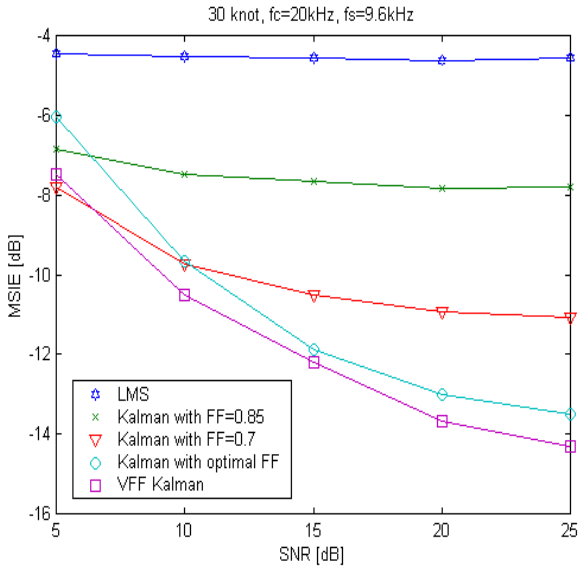

Fig. 2. MSIE comparision
(fc=20kHz, fs=9.6kHz, v=30 knots)

A digital technique for loudspeaker equalization

D. Lebrun[a], S.Debusne[a], S.Javelot[a], A.Landragin[b], G. de Rivoyre[b], J.Lewiner[a]

a- Laboratoire d'Electricité Générale, Ecole Supérieure de Physique et de Chimie Industrielles de la Ville de Paris, 10 rue Vauquelin, 75005 Paris, France

b- Cynove, 35 rue Tournefort, 75005 Paris

The natural responses of several loudspeaker systems have been measured with a precision microphone, in an anechoic chamber. These systems include small size or column type loudspeakers. The measured response is digitalized using a 24 bits converter. First a simulation is carried out using these data in order to evaluate and optimize the corrective algorithm. Second, the resulting algorithm is implemented in a DSP based unit in order to allow real time correction. In this paper, we will present the equalization technique and show the experimental results which have been obtained.

INTRODUCTION

The natural response of loudspeaker systems usually exhibits various defects over the whole audio frequency spectrum.[1] This is due to several factors. First, the loudspeakers themselves have not an ideal response. Second, more than one loudspeaker are usually needed in order to cover the full frequency range, typically from 50 to 20000 Hz. Passive filters are used to optimize the repartition of the electric signal to each loudspeaker. Unfortunately, these passive filters themselves also introduce some defects.

In order to optimize the overall response, we use a Digital Signal Processor (DSP) based unit. In a first step, we measure the impulse response of the loudspeaker system, in an anechoic chamber in order to obtain the required information[1]. Working in an anechoic chamber ensures that the measured parameters are related only to the loudspeaker system and not to the influence of the environment trough multiple reflections. In a second step, an equalization technique is implemented using the above parameters. Finally measurements are presented which show that the chosen algorithms ensure an almost perfect correction.

NATURAL RESPONSE OF THE LOUDSPEAKER SYSTEM

Measurement were carried out in an anechoic chamber using a low noise microphone and a digitalization unit, at a sampling rate of 48 kHz. The loudspeaker system is supplied with short pulses or fast rise time steps. Figure 1 shows a typical loudspeaker system response.

Defects are clearly visible on this response. The most visible one is the persistence of the signal up to 5 to 10 milliseconds.

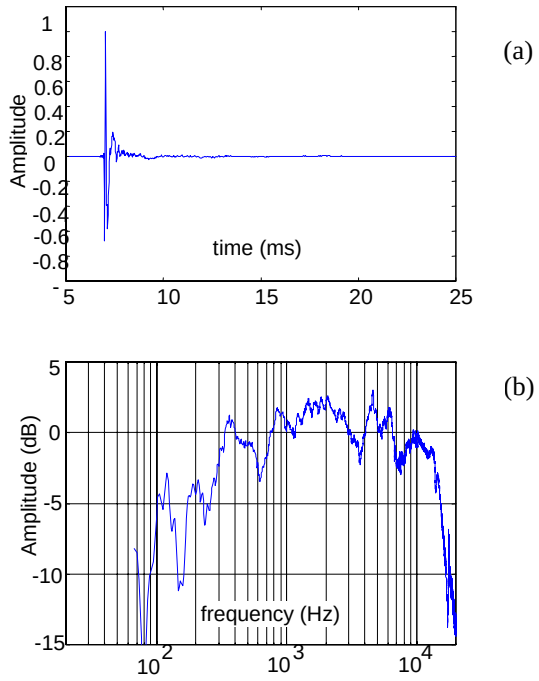

FIGURE 1 : Loudspeaker system -JMLAB 515- impulse response in time domain (a) and frequency domain (b)

THE EQUALIZATION TECHNIQUE

To equalize this response, we use a filtering method. We compared Finite Impulse Response (FIR) and Infinite Impulse Response (IIR) filters. The latter are difficult to stabilize and can present a nonlinear phase response. FIR filters are more stable, but require a larger number of filter taps to be efficient. However, we have chosen FIR filters because of the advantages associated with the good phase response and the superior stability[2][3].

In order to compute the different coefficients of this filter we define respectively $S(t)$ and $W(t)$ as the loudspeaker system and the filter responses. Let

$X(t)$ be the signal to be reproduced. The resulting sound pressure is expressed as :

$$p(t)=S(t)\otimes W(t)\otimes X(t) \qquad (1)$$

where $\otimes$ is the convolution operator. If the system were ideal, this pressure would be :

$$p_i(t)=I(t)\otimes X(t) \qquad (2)$$

where $I(t)$ is the identity, having a flat frequency response and a linear phase, in the considered frequency domain. Thus, the corrective steps must be such that

$$S(t)\otimes W(t)=I(t) \qquad (3)$$

which implies the deconvolution of $I(t)$ by $S(t)$. Figure 2 shows an example of computed 4000 taps filter that corrects the impulse response of figure 1.

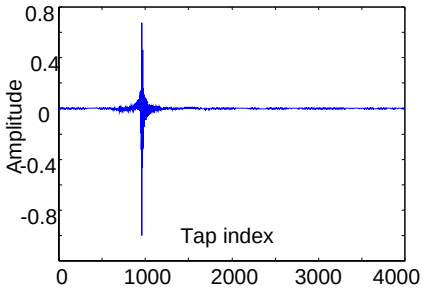

FIGURE 2 : $W(t)$ for the correction of the response shown in figure 1.

Figure 3 shows the theoretical impulse response of the loudspeaker system described in figure 1 and the above filter.

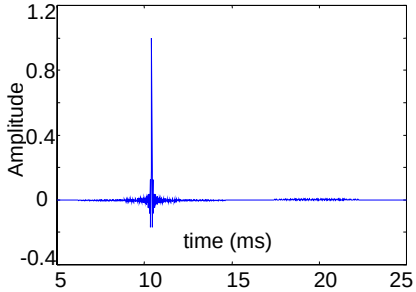

FIGURE 3 : Theoretical overall impulse response

We can see that the filter is quite efficient and can be implemented in an embedded electronic system.

EXPERIMENTAL RESULTS

To test the correction in real situations, we use a DSP based unit, well suited to perform fast convolutions even with a large number of filer taps. Furthermore, we used a low noise Digital to Analog Converter (DAC) and a low noise amplifier to supply the loudspeaker system with the signal generated by the DSP unit.

To evaluate the performance of the filter we measure the "corrected" impulse response, using the same measurement method that was used to measure the initial loudspeaker system impulse response. Figure 4 shows resulting pressure, in time domain (a) and in frequency domain (b).

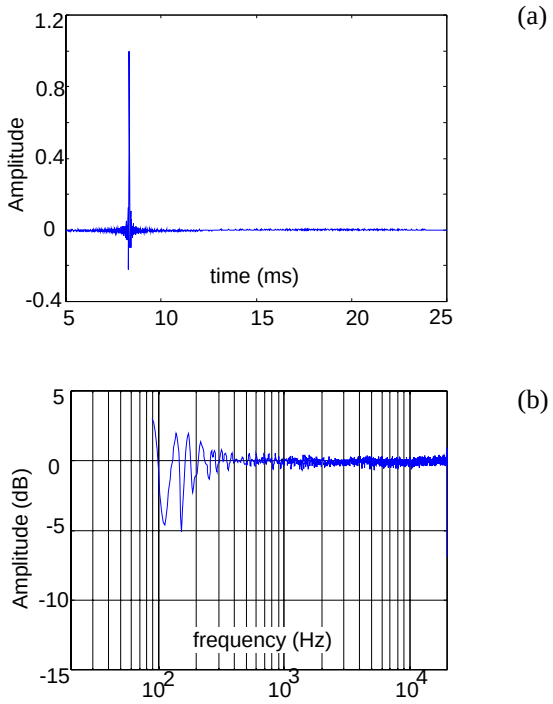

FIGURE 4 : Measured pressure, in time domain (a) and frequency domain (b)

The ripple is within 1 dB between 300 to 20000 Hz, and within 5-7 dB below 300 Hz.

CONCLUSION

In this paper, we present a digital technique for loudspeaker system equalization. We show that an embedded system can correct a loudspeaker system almost perfectly.

REFERENCES

1. See for instance Vance Dickason, *Enceintes Acoustiques & Haut-parleur*, Publitronic / Elecktor, Paris, 1996, p 161-225
2. J. Kuriyama, Y. Furukawa, *Adaptative Loudspeaker System*, J. Audio Eng. Soc. Vol 37, n°11 p 919-926.
3. P.A. Nelson & S.J. Elliott, *Active control of Sound*, Academic Press, San Diego, 1992, p 92-115